Broadband pulsed quadrature measurements with calorimeters

Ezad Shojaee,[1, 2, *] James R. van Meter,[1] Karl Mayer,[3] Scott Glancy,[1] and Emanuel Knill[1, 4]

[1] *National Institute of Standards and Technology, Boulder, Colorado 80305, USA*
[2] *Department of Physics, University of Colorado, Boulder, Colorado, 80309, USA*
[3] *Quantinuum, Broomfield, CO 80021*
[4] *Center for Theory of Quantum Matter, University of Colorado, Boulder, Colorado 80309, USA*

(Dated: November 21, 2025)

A fundamental problem in quantum optics is to measure a quadrature operator of a mode described by a shape in the time or frequency domain. This can be done by pulsed homodyne detection, in which the signal and a high-amplitude pulsed local oscillator (LO) interfere on a beam splitter whose output ports are monitored by photo-detectors. The quadrature value is proportional to the difference between the photo-detectors' signals. When the shape of the mode is too broad in frequency, the lack of uniform spectral response of detectors prevents direct application of this technique. We show that pulsed homodyne detection can be generalized to *broadband pulsed (BBP) homodyne detection* with detectors such as calorimeters that detect total energy instead of total photon number. This generalization has applications in measurements of femtosecond pulses and, speculatively, of Rindler modes. We analyze how the implemented measurement approaches an ideal quadrature measurement with growing LO amplitude, and prove that the moments of the measurement converge to the moments of the quadrature and that the measurement distributions converge weakly.

Homodyne detection is a method to measure quadrature operators of an optical signal, both in the frequency and time domains [1, 2]. In homodyne detection the signal interferes with a high-amplitude, mode-matched local oscillator (LO) on a balanced beam splitter. The light exiting the two output ports of the beam splitter is measured with two high-efficiency detectors such as photodiodes (Fig. 1), and the measurement result is obtained by scaling the difference between the detector outputs. This approaches an ideal quadrature measurement in the limit of large LO amplitudes. The LO can be continuous or pulsed. In continuous wave homodyne, the intensity difference is integrated against the temporal shape that defines the quadrature. Many quadratures can be measured simultaneously in this scheme if their spectra are within the detector's bandwidth. In pulsed homodyne, the LO is pulsed with a shape that matches that of the quadrature of interest. Only the quadrature matching the LO is measured, but the detectors need not be time-resolving, and the LO power can be concentrated where it is needed. Pulsed homodyne is required when slow detectors, such as calorimeters, are used.

Standard pulsed homodyne detection requires the detector output to be proportional to the total number of photons arriving during the pulse. This restricts the bandwidth of the LO pulse and of the optical signal during the pulse to a spectral band over which the detectors have nearly uniformly high efficiency. In practice, noisy, high-efficiency photon counters are used, and if the noise increases at a sublinear rate with photon number, a good quadrature measurement can still be obtained by increasing the LO amplitude. There are no detectors with a wide enough spectral band to measure quadratures of optical signals with octave-spanning bandwidth such as those associated with femtosecond pulses. Such octave-spanning quadratures are also of interest in studies of the Unruh effect [3], which arises for accelerating observers due to the non-zero temperature of Rindler modes, which are extremely broadband in an inertial frame.

One type of detector with the potential for high-efficiency detection over a broad frequency band is the calorimeter. Rather than counting photons, calorimeters record the total energy. As a result, photons of different energy contribute by different amounts to the calorimeter output. For example the calorimeter records the same value for two photons of energy $1/2$ and one photon of energy 1 in arbitrary units. Calorimeters are widely used and can achieve near-unit efficiency for measuring energy across the spectrum. For instance, transition edge sensors (TES) directly detect the change of temperature due to incident light on a superconducting island at the transition temperature [4, 5] and have the potential for high efficiency over a wide bandwidth [6, 7].

To enable the use of detectors such as calorimeters to measure specific quadratures of broadband modes, we introduce *broadband pulsed (BBP) homodyne detection*, a generalization of standard pulsed homodyne detection. BBP homodyne is based on detectors that record observables, such as total energy, that are expressed as linear combinations of photon numbers in the modes of an orthogonal-mode basis. As in standard pulsed homodyne, the BBP homodyne measurement result is the scaled difference between the detector outputs. We show that arbitrary quadratures expressible in this mode basis can be measured with a high-amplitude LO whose pulse shape is determined by the quadrature of interest. A feature of BBP homodyne is that the mode of the LO is typically different from the mode whose quadrature one wishes to measure. For all homodyne detection methods, convergence of the measurement outcomes to ideal measurements of the quadrature depends on the type of convergence under consideration and the state. Convergence can fail for pathological states. Standard pulsed homodyne satisfies that the moments of the measurement outcomes converge to those of the quadrature when these moments are finite, see Ref. [8]. Less well known is that the measurement distribution converges weakly, which is defined as convergence of expectation values of continuous bounded functions of the measurement outcomes. We prove that BBP homodyne detection satisfies moment convergence and apply the general theory relating the convergence of moments to weak convergence, developed by [9, 10] to prove weak convergence.

To start the analysis, we denote generic modes of a field by $a, b, \ldots$ and the corresponding mode (annihilation) operators by $\hat{a}, \hat{b}, \ldots$ with or without indices. Mode operators satisfy $\left[\hat{a}, \hat{a}^\dagger\right] = 1$. In the physical field's state space, $\hat{a}$ annihilates the vacuum, and $\hat{a}^\dagger$ applied to the vacuum creates a photon in mode a with a particular wavefunction in momentum space. The vacuum state of a mode is denoted by $|0\rangle$. The state space of a mode is the Hilbert space spanned by the number states $|n\rangle = \left(\hat{a}^\dagger\right)^n |0\rangle / \sqrt{n!}$. We use the convention that generalized quadratures of mode a are defined by operators $\hat{q}_{a,\alpha} = -i(\alpha\hat{a}^\dagger - \alpha^*\hat{a})$ where α is a complex number. A coherent state is a normalized state $|\beta\rangle$ that satisfies $\hat{a}|\beta\rangle = \beta|\beta\rangle$. This identity determines $|\beta\rangle$ up to a global phase. Having fixed the normalized vacuum state $|0\rangle$, we fix the phase by requiring that $\langle\beta|0\rangle$ is positive real.

The configuration for pulsed homodyne is shown in Fig. 1, where for standard pulsed homodyne, the detectors count total number of photons. The full state space of the signal is that of N modes $\boldsymbol{a}$ with mode operators $\hat{\boldsymbol{a}}$. The goal is to measure the generalized quadrature $\hat{q}_{\boldsymbol{a},\boldsymbol{\beta}}$ (target quadrature). For this purpose an LO is introduced on a family of modes $\boldsymbol{b}$, each of which is matched to the corresponding signal mode. To approximately measure a generalized quadrature of the modes, the LO state is the coherent state $|R\boldsymbol{\beta}\rangle_{\boldsymbol{b}}$, where R is a large real number. It is convenient to explicitly introduce the displacement operator $\hat{D}_{\boldsymbol{b},R\boldsymbol{\beta}}$ that makes this state from vacuum, as shown in the figure. The initial state consists of the signal state $\rho_{\boldsymbol{a}}$ on the signal modes $\boldsymbol{a}$, and vacuum $\boldsymbol{0_b}$ on the LO modes $\boldsymbol{b}$. The signal modes and the matching LO modes are combined on a balanced beam splitter. The outgoing modes, $\boldsymbol{c}$ and $\boldsymbol{d}$ can be expressed in terms of the original signal and the pre-displacement LO modes as follows:

$$\hat{\boldsymbol{c}} = \frac{1}{\sqrt{2}}\left(\hat{\boldsymbol{a}} + \hat{\boldsymbol{b}} + R\boldsymbol{\beta}\right),$$
$$\hat{\boldsymbol{d}} = \frac{1}{\sqrt{2}}\left(\hat{\boldsymbol{a}} - \hat{\boldsymbol{b}} - R\boldsymbol{\beta}\right). \tag{1}$$

Here we made a particular sign and phase choice for the balanced beam splitter. The homodyne configuration is completed by photon counting on each of the two outgoing arms of the beam splitter, subtracting the counts obtained, and dividing by R. To describe this measurement, we subtract the scaled total photon number operators for the arms to obtain the measurement operator

$$\begin{aligned}\hat{h} &= \frac{1}{R}\left(\hat{n}_{\boldsymbol{c}} - \hat{n}_{\boldsymbol{d}}\right)\\ &= \frac{1}{R}\left(\hat{\boldsymbol{c}}^\dagger\cdot\hat{\boldsymbol{c}} - \hat{\boldsymbol{d}}^\dagger\cdot\hat{\boldsymbol{d}}\right)\\ &= \boldsymbol{\beta}\cdot\hat{\boldsymbol{a}}^\dagger + \boldsymbol{\beta}^*\cdot\hat{\boldsymbol{a}} + \frac{1}{R}\left(\hat{\boldsymbol{a}}^\dagger\cdot\hat{\boldsymbol{b}} + \hat{\boldsymbol{b}}^\dagger\cdot\hat{\boldsymbol{a}}\right).\end{aligned} \tag{2}$$

Here "·" denotes the inner product between two vectors, and complex conjugation and dagger is applied elementwise. Intuitively, for large R the summand with a factor of $\frac{1}{R}$ can be neglected, so $\hat{h}$ approaches a measurement of the target quadrature $\hat{q}_{\boldsymbol{a},i\boldsymbol{\beta}}$. We should note that the deviation of $\hat{h}$ from the target quadrature measurement is affected by the state of photons in modes orthogonal to that of the target quadrature. The amplitude R needs to be increased to make the signal from such photons

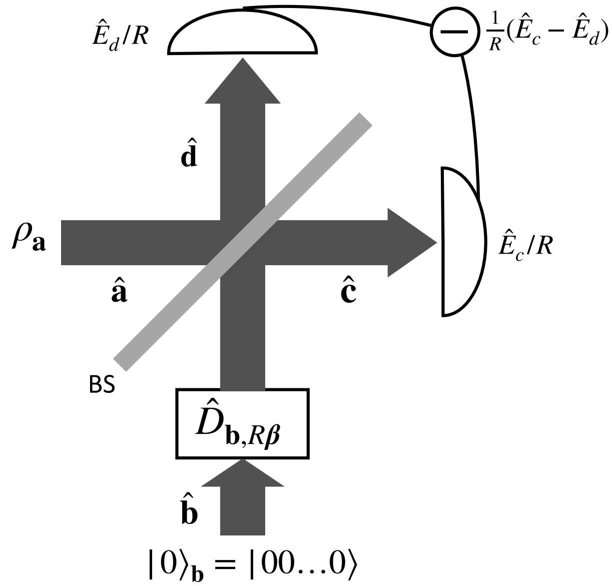

FIG. 1. Multi-mode homodyne measurement configuration. The signal modes enter from the left on modes $\boldsymbol{a}$ with mode operators $\hat{\boldsymbol{a}}$. The LO modes enter from the bottom on modes $\boldsymbol{b}$. The LO modes are initially in vacuum, and the LO coherent state is explicitly prepared by the displacement operator $\hat{D}_{\boldsymbol{b},R\beta}$. Modes $\boldsymbol{a}$ and $\boldsymbol{b}$ are combined on a balanced beam splitter(BS). The beam splitter's outgoing modes, $\boldsymbol{c}$ and $\boldsymbol{d}$ are measured with photon counters in standard pulsed homodyne or calorimeters in BBP pulsed homodyne. In both cases the observable associated with the detector is of the form $\hat{E} = \sum_k \omega_k \hat{f}_k^\dagger \hat{f}_k$ with $\boldsymbol{f} = \boldsymbol{c}$ or $\boldsymbol{d}$. For standard pulsed homodyne, $\omega_k = 1$ for all k. For BBP homodyne, ω_k is the energy of photons in the k'th mode. The homodyne measurement result is determined by subtracting one detector's output from the other and rescaling the result by a factor of $1/R$. In general, ω_k can be arbitrary positive weights.

negligible.

In BBP homodyne, an ideal calorimeter measures the energy operator

$$\hat{E} = \sum_{k=1}^{N} \omega_k \hat{a}_k^\dagger \hat{a}_k. \tag{3}$$

where ω_k is the energy of a photon in mode k. It is worth noting that our treatment does not require ω_k to be the energy of a mode k. It can be an arbitrary real, positive weight. If $\omega_k = 1$ for all k, $\hat{E}$ measures the total photon number. We therefore refer to the vector $\boldsymbol{\omega}$ as mode weights.

Consider the homodyne setup with calorimeters instead of photon counters at the outgoing arms of the balanced beam splitter. The measurement operator corresponding to subtracting the calorimeter measurement results and dividing by R is

$$\begin{aligned} \frac{1}{R}\Delta\hat{E} &= \frac{1}{R}\sum_{k=1}^{N} \omega_k \big(\hat{c}_k^\dagger \hat{c}_k - \hat{d}_k^\dagger \hat{d}_k\big) \\ &= \sum_{k=1}^{N} \omega_k (\hat{a}_k^\dagger \beta_k + \beta_k^* \hat{a}_k) + \frac{1}{R}\sum_{k=1}^{N} \omega_k (\hat{a}_k^\dagger \hat{b}_k + \hat{b}_k^\dagger \hat{a}_k). \end{aligned} \tag{4}$$

Here all operators represent incoming mode operators according to Heisenberg evolution. In particular $\Delta\hat{E}$ when so expressed depends on the LO displacement and therefore on R. Assuming that the contribution from terms multiplied by $\frac{1}{R}$ is negligible, this approaches a measurement of the target generalized quadrature $\hat{q}_{\boldsymbol{a},i(\boldsymbol{\omega}*\boldsymbol{\beta})}$, where "*" denotes the element-wise product defined by $(\boldsymbol{\gamma} * \boldsymbol{\gamma}')_k = \gamma_k \gamma'_k$. From now on, we omit the mode label on operators such as $\hat{q}$ when the modes are clear from context. If we wish to measure the generalized coordinate $\hat{q}_{\boldsymbol{\alpha}}$, we choose $\boldsymbol{\beta} = -i\boldsymbol{\alpha} * (1/\boldsymbol{\omega})$, where $1/\boldsymbol{\omega}$ is the vector with k'th entry $1/\omega_k$. The required LO amplitude is $R\boldsymbol{\beta} = -i\boldsymbol{\alpha} * (R/\boldsymbol{\omega})$.

In our treatment, quadrature expectations and coherent state amplitudes are unitless and scaled so that the vacuum expectation of the square of a normalized quadrature is 1/2. The units of the weights $\boldsymbol{\omega}$ and of the scale R are therefore identical. In the case of calorimeters, they both have the same energy units. For the purposes of BBP homodyne, quantities of interest depend on R and $\boldsymbol{\omega_k}$ only through ratios such as R/ω_k. The vector $\boldsymbol{\beta}$ describes the shape of the LO, but as defined, carries inverse energy units. While not necessary for our treatment below, we can can order the modes by energy, so that ω_1 is the maximum mode energy. The basic unnormalized mode shape may then be defined as $\boldsymbol{\beta}_0 = \omega_1\boldsymbol{\beta}$. Then R/ω_1 is a unitless scale defining the amplitude of the LO. For standard pulsed homodyne, $\boldsymbol{\beta}_0 = \boldsymbol{\alpha}$ and R/ω_1 is the conventional LO amplitude.

Define $\delta = 1/R$ and introduce the BBP measurement operator

$$\begin{aligned} \hat{q}_{\boldsymbol{\alpha},\delta} &= \delta\Delta\hat{E} \\ &= \hat{q}_{\boldsymbol{a},\boldsymbol{\alpha}} + \delta\Big(\big(\boldsymbol{\omega} * \hat{\boldsymbol{a}}^\dagger\big)\cdot\hat{\boldsymbol{b}} + \big(\boldsymbol{\omega} * \hat{\boldsymbol{b}}^\dagger\big)\cdot\hat{\boldsymbol{a}}\Big). \end{aligned} \tag{5}$$

As noted previously $\Delta\hat{E}$ is defined as an operator on the incoming modes and therefore depends on δ through the displacement on the LO modes. The associated LO amplitudes are

$$\boldsymbol{\beta}_{\mathrm{LO},\boldsymbol{\alpha},\delta} = -i\boldsymbol{\alpha} * \frac{1}{\boldsymbol{\omega}}. \tag{6}$$

The LO with these amplitudes can be obtained by pulse shaping. Suitable pulse shaping techniques have been developed for femtosecond pulses. For example, see the review [11]. We define $\hat{q}_{\boldsymbol{\alpha},0} = \hat{q}_{\boldsymbol{a},\boldsymbol{\alpha}}$. When $\boldsymbol{\alpha}$ is clear from context, we abbreviate $\hat{q}_\delta = \hat{q}_{\boldsymbol{\alpha},\delta}$ and $\hat{q} = \hat{q}_{\boldsymbol{\alpha},0}$.

The BPP measurement operator $\hat{q}_\delta$ is by design proportional to a difference of two commuting total energy operators at the outgoing modes, so the spectrum of $\hat{q}_\delta$ is discrete. The outgoing mode Fock states that diagonalize the energy operators correspond to displaced Fock states in the incoming modes, where the displacement diverges to infinity as δ goes to zero. In contrast, $\hat{q}$ has continuous spectrum and improper eigenspaces associated with its spectral measure. This immediately suggests that the convergence of q_δ to the target quadrature q_0 is not straightforward. The BBP measurement operator is unbounded, as is the quadrature measurement. As a result, there are states in the Hilbert space not in the domains of these operators, and for such states convergence is impossible. Thus proofs and quantification of convergence are necessarily state-dependent.

The BBP homodyne configuration, as described above, has perfect calorimeters. However, as with the standard homodyne configuration, noisy but high-efficiency calorimeters can be used, provided that the noise scales sublinearly with total energy.

Our first convergence result establishes that the moments for BBP homodyne measurement outcome distributions converge to the moments of the target quadrature. This result is well known for standard homodyne, for example, see Ref. [12], Eq. (3.2) and following, or Ref. [9] Prop. 8. The proofs for standard homodyne generalize with little modification to BBP homodyne. We use the angle-bracket notation $\langle\cdot\rangle_\rho$ for expectations of operators with respect to state ρ. We omit the subscript when the state with respect to which expectations are computed is clear from context.

Theorem 1. *Suppose the state $\rho_{\boldsymbol{a}}$ on the signal modes $\boldsymbol{a}$ has well-defined expectations for all polynomials in the mode operators and their adjoints up to degree n, and the joint initial state is $\rho_{\boldsymbol{a}} \otimes \mathbf{0}_{\boldsymbol{b}}$. Then the moments of $\hat{q}_\delta$ and*

$\hat{q}$ satisfy

$$\langle \hat{q}_\delta^n \rangle = \langle \hat{q}^n \rangle + O(\delta^2), \tag{7}$$

where the constant in the order notation depends on $\rho_{\boldsymbol{a}}$.

The proof is provided in App. A. The first moment does not depend on δ and is identical to the target quadrature's. Because the pre-displacement LO modes are in vacuum, one can show that for the second moment we have $\langle \hat{q}_\delta^2 - \hat{q}^2 \rangle = \delta^2 \sum_k \omega_k^2 \langle \hat{n}_{a_k} \rangle$ If it is known that the signal state is Gaussian, then it is sufficient to measure the first and second moments of its quadratures. The above shows that the second moments of $\hat{q}_\delta$ are biased high by a term of order δ^2 with a coefficient that can be estimated knowing only bounds on the expected photon numbers.

Theorem 1 applies specifically to states with well-defined expectations for all polynomials of mode operators. A dense linear space of pure states with such well-defined expectations is the set $\mathcal{D}_S$ of Schwartz states, defined as states whose Wigner functions decay super-polynomially [13]. This set of states is preserved by all polynomials of the mode operators and their adjoints. It includes number states and coherent states and their finite linear combinations.

Next we show that the moment convergence for a restricted family of signal states in Thm. 1 implies that for every bounded continuous function f of the reals and every signal state, the expectations of $f(\hat{q}_\delta)$ with respect to the BBP homodyne outcome distributions converge to the expectation of $f(\hat{q})$. This property is equivalent to weak convergence in the sense of probabilities of the positive operator valued measures (POVMs) realized by BBP homodyne to the spectral measure of $\hat{q}$ (see [9] Prop. 3).

Theorem 2. *For every continuous complex-valued bounded function f on the reals and for every state $\rho = \rho_{\boldsymbol{a}} \otimes \mathbf{0}_{\boldsymbol{b}}$, we have*

$$\lim_{\delta\to 0} \langle f(\hat{q}_\delta) \rangle = \langle f(\hat{q}) \rangle. \tag{8}$$

The proof is provided in App. B. There are many equivalent definitions for weak convergence of the measures associated with $\hat{q}_\delta$ to the measures of $\hat{q}$. The version given in Thm. 2 corresponds to Ref. [9] Prop. 3 (iv), which is also equivalent to the convergence of overlaps as expressed in the following corollary.

Corollary 3. *Let $\boldsymbol{g}$ be any family of modes or other quantum systems that are not involved in the BBP homodyne measurements, and f a continuous complex-valued bounded function on the reals. For all joint pure states $|\phi\rangle$ and $|\psi\rangle$ of $\boldsymbol{g}$, the signal, and the LO modes, if $|\phi\rangle$ and $|\psi\rangle$ are vacuum on the LO modes, then we have*

$$\lim_{\delta\to 0} \langle \phi | f(\hat{q}_\delta) | \psi \rangle = \langle \phi | f(\hat{q}) | \psi \rangle, \tag{9}$$

and

$$\lim_{\delta\to 0} |(f(\hat{q}_\delta) - f(\hat{q})) |\psi\rangle| = 0. \tag{10}$$

The proof of this corollary is provided in App. C. Eq. (10) can be interpreted as strong convergence of $f(\hat{q}_\delta)$ to $f(\hat{q})$ on the subspace of states that are vacuum on the LO modes.

Discussion. BBP homodyne can be seen to be a generalization of standard pulsed homodyne by setting all the weights to $\omega_k = 1$. The well-known properties of standard pulsed homodyne are preserved. In particular, the moments of the BBP homodyne observables converge to the moments of the target quadrature and the distributions of BBP measurement outcomes converge weakly to that of the target quadrature.

The main motivation for introducing BBP homodyne is to use calorimeters to measure quadratures of broadband modes such as those present in optical femtosecond pulses or modes of interest in quantum field theory such as Rindler modes. In principle, it is possible to perform broadband quadrature measurements by the means of a Bragg grating or similar device to separate the spectral components of the light, parallel measurement of narrowband quadratures, and combination of the results in software. Another proposal is to use broad-band parametric amplification followed by a direct measurement of the spectrum [14]. BBP homodyne has the advantage of a simple experimental setup requiring only one beam splitter and two broadband calorimeters, in addition to the LO. The calorimeters need not resolve time and can be slow. In particular, there is no requirement for high-speed readout.

In our treatment of BBP homodyne, we assumed ideal calorimeters. Balanced losses in the calorimeters can be handled as is done for standard pulsed homodyne. Such losses can be treated as losses in the signal state before the beam splitter and a change of the LO. In many measurements, the effect of such loss can be inverted or accounted for. See Ref. [15] for a treatment of losses in standard homodyne. Another approach is to directly determine the POVMs associated with photon number outcomes asin the theory of operational homodyne [12, 16] and express expectations of mode operators in terms of the POVM expectations. Such techniques are applicable when the LO is weak and are used in weak-field homodyne, for example, see Refs. [17, 18]. In standard homodyne with balanced photodiodes, the photodiodes have constant added noise whose effect on the quadrature measurements is suppressed by high LO amplitudes, see, for example, [19, 20]. The same holds for BBP homodyne with calorimeters that have energy-independent added noise such as might be expected from imperfect energy resolution.

Further work is required to quantify the convergence of the measurement outcome distribution to the ideal one for the target quadrature for both standard homodyne and BBP homodyne. The expression given after the Thm. 1 quantifies the convergence of only the second moment. In the analysis of standard homodyne, besides quantifying convergence for special families of states such as in Ref. [12], convergence arguments are limited to asymptotic analysis and recommendations for LO energies large compared to the expected photon number in the signal, for example see Refs. [8, 21]. Quantified convergence would be helpful in many quantum information applications where the fidelities of measurement distributions and states remaining in unmeasured modes matters. Examples include CV quantum teleportation [22, 23] and CV quantum computing [24].

Regarding the application of BBP homodyne in characterization of the Rindler modes, it is necessary to determine how to realize the local oscillator and beam splitter while maintaining the compatibility with the relativistic quantum field under investigation. Because it is impossible to measure standard, single-frequency Rindler modes, it is also necessary to determine how to reveal the desired quadrature information from smeared such modes. Relevant suggestions have been offered for different detection systems in [25].

Acknowledgments. We thank Adriana Lita for help with identifying and describing the performance of broadband TES detectors. We also thank Zachary Levine and Michael Mazurek for assistance with reviewing the paper before submission. E. S and J. R. v. M. acknowledge support from the Professional Research Experience Program (PREP) operated jointly by NIST and the University of Colorado. This work includes contributions of the National Institute of Standards and Technology, which are not subject to U.S. copyright.

* Current address: IonQ, College Park, MD 20740

[1] G. Breitenbach, S. Schiller, and J. Mlynek. Measurement of the quantum states of squeezed light. *Nature*, 387(6632):471–475, 1997.
[2] D. T. Smithey, M. Beck, M. G. Raymer, and A. Faridani. Measurement of the Wigner distribution and the density matrix of a light mode using optical homodyne tomography: Application to squeezed states and the vacuum. *Phys. Rev. Lett.*, 70:1244–1247, Mar 1993.
[3] Luís C. B. Crispino, Atsushi Higuchi, and George E. A. Matsas. The Unruh effect and its applications. *Rev. Mod. Phys.*, 80:787, 2008.
[4] K. D. Irwin. An application of electrothermal feedback for high resolution cryogenic particle detection. *Applied Physics Letters*, 66(15):1998–2000, 1995.
[5] K. D. Irwin, S. W. Nam, Blas Cabrera, B. Chugg, and Betty A. Young. A quasiparticle-trap-assisted transition-edge sensor for phonon-mediated particle detection. *Review of Scientific Instruments*, 66(11):5322–5326, 1995.
[6] B. Cabrera, R. M. Clarke, P. Colling, A. J. Miller, S. Nam, and R. W. Romani. Detection of single infrared, optical, and ultraviolet photons using superconducting transition edge sensors. *Applied Physics Letters*, 73(6):735–737, 1998.
[7] Kaori Hattori, Toshio Konno, Yoshitaka Miura, Sachiko Takasu, and Daiji Fukuda. An optical transition-edge sensor with high energy resolution. *Superconductor Science and Technology*, 35(9):095002, 2022.
[8] Samuel L. Braunstein. Homodyne statistics. *Physical Review A*, 42(1):474, 1990.
[9] J. Kiukas and P. Lahti. On the moment limit of quantum observables, with an application to the balanced homodyne detection. *Journal of Modern Optics*, 55(7):1175–1198, 2008.
[10] Jukka Kiukas. *Moment operators of observables in quantum mechanics, with applications to quantization and homodyne detection*. PhD thesis, University of Turku, Finland, 2008.
[11] Andrew M Weiner. Femtosecond pulse shaping using spatial light modulators. *Review of scientific instruments*, 71(5):1929–1960, 2000.
[12] Tomáš Tyc and Barry C. Sanders. Operational formulation of homodyne detection. *J. Phys. A: Math. Gen.*, 37:7341, 2004.
[13] Felipe Hernández and C. Jess Riedel. Rapidly decaying Wigner functions are Schwartz functions. *Journal of Mathematical Physics*, 63(2):022104, 2022.
[14] Yaakov Shaked, Yoad Michael, Z. Vered, Rafi, Leon Bello, Michael Rosenbluh, and Avi Pe'er. Lifting the bandwidth limit of optical homodyne measurement with broadband parametric amplification. *Nature communications*, 9(1):609, 2018.
[15] U Leonhardt and H Paul. Realistic optical homodyne measurements and quasiprobability distributions. *Physical Review A*, 48(6):4598, 1993.
[16] Konrad Banaszek and Krzysztof Wódkiewicz. Operational theory of homodyne detection. *Phys. Rev. A*, 55:3117–3123, Apr 1997.
[17] Werner Vogel. Homodyne correlation measurements with weak local oscillators. *Physical Review A*, 51(5):4160, 1995.
[18] Arik Avagyan. *Quantum State Characterization Using Measurement Configurations Inspired by Homodyne Detection*. PhD thesis, University of Colorado, Boulder, 2023. arXiv preprint arXiv:2305.19397.
[19] Hauke Hansen, T Aichele, C Hettich, P Lodahl, AI Lvovsky, J Mlynek, and S Schiller. Ultrasensitive pulsed, balanced homodyne detector: application to time-domain quantum measurements. *Optics Letters*, 26(21):1714–1716, 2001. arXiv:quant-ph/0104084.
[20] Thomas Gerrits, S Glancy, and Sae Woo Nam. A balanced homodyne detector and local oscillator shaping for measuring optical schrödinger cat states. In *Advanced Photon Counting Techniques V*, volume 8033, pages 262–268. SPIE, 2011.
[21] Joshua Combes and Austin P Lund. Homodyne measurement with a schrödinger cat state as a local oscillator. *Physical Review A*, 106(6):063706, 2022. arXiv:2207.10210.
[22] Samuel L. Braunstein and H. J. Kimble. Teleportation of continuous quantum variables. *Phys. Rev. Lett.*, 80:869–872, Jan 1998.
[23] A. Furusawa, J. L. Sørensen, S. L. Braunstein, C. A. Fuchs, H. J. Kimble, and E. S. Polzik. Unconditional quantum teleportation. *Science*, 282(5389):706–

709, 1998.
[24] Daniel Gottesman, Alexei Kitaev, and John Preskill. Encoding a qubit in an oscillator. *Phys. Rev. A*, 64:012310, Jun 2001.
[25] S. Jay Olson and Timothy C. Ralph. Entanglement between the future and the past in the quantum vacuum. *Phys. Rev. Lett.*, 106:110404, 2011.
[26] R. V. Kadison and J. R. Ringrose. *Fundamentals of Theory of Operator Algebras. Vol. I: Elementary Theory*, volume 15 of *Graduate Studies in Mathematics*. American Mathematical Society, Providence, RI, 1997.
[27] Michael. Reed and Barry Simon. *Methods of Modern Mathematical Physics*, volume 1. Functional Analysis. Academic Press, New York, NY, 1980.

Appendix A. Proof of Theorem 1

Proof. Define the operator $\hat{C} = (\hat{q}_\delta - \hat{q})/\delta = \Big(\boldsymbol{\omega} * \hat{\boldsymbol{a}}^\dagger\Big) \cdot \hat{\boldsymbol{b}} + \Big(\boldsymbol{\omega} * \hat{\boldsymbol{b}}^\dagger\Big) \cdot \hat{\boldsymbol{a}}$, which does not depend on δ. We expand $\hat{q}_\delta^n = (\hat{q} + \delta\,\hat{C})^n$ as a sum of 2^n monomials expressed as ordered products of $\hat{q}$ and $\delta\,\hat{C}$. We can order the monomials by the power of δ that multiplies them. Let $\hat{Q}_k$ be the sum of the monomials that are multiplied by δ^k, so $\hat{q}_\delta^n = \sum_{k=0}^n \hat{Q}_k$. Then $\hat{Q}_0 = \hat{q}^n$, so $\langle \hat{Q}_0 \rangle = \langle \hat{q}^n \rangle$ contributes the first term on the right-hand side of Eq. (7). We can express $\hat{Q}_1$ as

$$\hat{Q}_1 = \delta \sum_{k=0}^{n-1} \hat{q}^k \hat{C} \hat{q}^{n-k-1}. \tag{A.1}$$

The factors of $\hat{q}$ in the sum act only on the signal modes $\boldsymbol{a}$, and $\hat{C}$ is linear in the LO mode operators. Since ρ is vacuum on the pre-displacement LO modes, the expectations of the summands of $\hat{Q}_1$ are zero. Consequently $\langle \hat{Q}_1 \rangle = 0$. The remaining terms in the expansion are multiplied by a factor of order δ^2 or smaller. Their expectations may be expressed as expectations of monomials of degree at most n in the signal mode operators and their adjoints, and of degree at most n in the LO mode operators and their adjoints. Taking account of the vacuum state in the LO mode, these expectations reduce to expectations of $\rho_{\boldsymbol{a}}$ of monomials of degree at most n in the signal mode operators. The expectations of these monomials are finite by assumption and do not depend on δ. Thus

$$\begin{aligned} \langle \hat{q}_\delta^n \rangle &= \sum_{k=0}^{n} \langle \hat{Q}_k \rangle \\ &= \langle \hat{Q}_0 \rangle + \langle \hat{Q}_1 \rangle + O(\delta^2) \\ &= \langle \hat{q}^n \rangle + O(\delta^2). \end{aligned} \tag{A.2}$$

□

APPENDIX B. PROOF OF THEOREM 2

Proof. To prove the theorem we implement a version of the sequence of steps given in Sect. 4 of Ref. [9] for establishing weak convergence for measurement schemes. In this reference, the steps are implemented to prove weak convergence of standard homodyne with one mode. The first step is to identify a dense subspace of states on which the target quadrature's measurement outcome distribution is determined by its moments (Ref. [9] Def. 2). A probability distribution μ on the reals is determined by its moments if for every probability distribution ν whose moments are the same as those of μ, we have $\mu = \nu$. The set $\mathcal{D}_{\rm coh} \subseteq \mathcal{D}_S$ of finite linear combinations of coherent states suffices for this purpose. For one mode, this is a consequence of Ref. [9] Lemma 2. Because $\hat{q}$ is the quadrature of one mode, this Lem. 2 suffices for BBP homodyne. See also the discussion after Proposition 2 in the reference. The next step is to verify that for states in $\mathcal{D}_{\rm coh}$, the positive-operator-valued measures (POVMs) associated with $\hat{q}_\delta$ have moments converging to those of $\hat{q}$. For BBP homodyne, since $\mathcal{D}_{\rm coh}$ is a subset of the set of Schwartz states, this is a consequence of Thm. 1. For the purpose of applying the results of Ref. [9], the POVMs associated with $\hat{q}_\delta$ are the POVMs on the signal modes obtained from the projection-valued measures of the operators $\hat{q}_\delta$ by fixing the pre-displacement state of the LO modes to be vacuum. The POVM for $\hat{q}$ is projection-valued, but the POVMs for $\hat{q}_\delta$ are not, they are positive-operator valued and referred to as "semispectral measures" in Ref. [9]. With this, the conditions of Ref. [9] Prop. 5 are satisfied. That is, with the definitions of this reference, because of moment convergence, there is a POVM that is a moment limit of the POVMs associated with $\hat{q}_\delta$. One such moment limit is the spectral measure of $\hat{q}$. Since the latter is determined by its moments, this moment limit is unique. The conclusion from the reference's Prop. 5 is that the POVMs associated with $\hat{q}_\delta$ converge weakly in the sense of probabilities to the spectral measure of $\hat{q}$. This is equivalent to the conclusion of our theorem. □

APPENDIX C. PROOF OF COROLLARY 3

Proof. To prove Eq. (9), for any complex, bilinear form $\langle\phi|\,\hat{A}\,|\psi\rangle$ with bounded operator $\hat{A}$,

$$\begin{aligned} \langle\phi|\,\hat{A}\,|\psi\rangle &= \frac{1}{4}\sum_{j=0,1,2,3} (-i)^j (\langle\phi| + (-i)^j\,\langle\psi|)\hat{A}(|\phi\rangle + i^j\,|\psi\rangle) \\ &= \frac{1}{4}\sum_{j=0,1,2,3} (-i)^j\,\langle\rho_j|\,\hat{A}\,|\rho_j\rangle\,, \end{aligned} \tag{C.1}$$

where $|\rho_j\rangle = |\phi\rangle + i^j\,|\psi\rangle$. We can re-express $\langle\rho_j|\,\hat{A}\,|\rho_j\rangle = \mathrm{tr}\Big(|\rho_j\rangle\!\langle\rho_j|\,\hat{A}\Big)$. After substituting $\hat{A} = f(\hat{q}_\delta)$ and tracing out systems other than the signal and LO modes in the state $|\rho_j\rangle\langle\rho_j|$, we can apply Thm. 2 to complete the proof of the corollary. The identity in Eq. (C.1) is an instance of the polarization identity, a textbook method used to reconstruct an inner product from the associated norm, for instance see [26, 27].

To prove Eq. (10), consider the quantity

$$
\begin{aligned}
&|(f(\hat{q}_\delta) - f(\hat{q}))\,|\psi\rangle|^2 \\
&\quad = \langle\psi|\, f(\hat{q}_\delta)^\dagger f(\hat{q}_\delta)\,|\psi\rangle + \langle\psi|\, f(\hat{q})^\dagger f(\hat{q})\,|\psi\rangle \\
&\qquad - 2\,\mathrm{Re}(\langle\psi|\, f(\hat{q}_\delta)^\dagger f(\hat{q})\,|\psi\rangle).
\end{aligned}
\tag{C.2}
$$

Since $\hat{q}$ is self-adjoint, we have $f(\hat{q})^\dagger = f^*(\hat{q})$. Substituting $f^*(x)f(x)$ for $f(x)$ and $\langle\psi|$ for $\langle\phi|$ in Eq. (9) shows that the first summand on the right-hand side of Eq. (C.2) converges to the second summand. Substituing $f^*(x)$ for $f(x)$, $\langle\psi|$ for $\langle\phi|$ and $f(\hat{q})\,|\psi\rangle$ for $|\psi\rangle$ in Eq. (9) shows that the third summand converges to $2\,\mathrm{Re}(\langle\psi|\, f(\hat{q})^\dagger f(\hat{q})\,|\psi\rangle) = 2\,\langle\psi|\, f(\hat{q})^\dagger f(\hat{q})\,|\psi\rangle$. For this we take advantage of the fact that $f(\hat{q})\,|\psi\rangle$ is also vacuum on the LO modes. Adding up the limit of each summand therefore gives 0. □